*Journal of Mining and Environment (JME) Vol. 16, No. 3, 2025, 925-946*

Shahrood University of Technology

**Journal of Mining and Environment (JME)**

*Journal homepage: www.jme.shahroodut.ac.ir*

Iranian Society of Mining Engineering (IRSME)

# Integrated Slope Stability Assessment and Solutions using PLAXIS 2D and GEO5

Sahil Thakur* and Ravi Kumar Sharma

*Department of Civil Engineering, National Institute of Technology Hamirpur, Himachal Pradesh, India*

**Article Info**

*Received 9 December 2024*

*Received in Revised form 9 February 2024*

*Accepted 8 March 2024*

*Published online 8 March 2024*

DOI: 10.22044/jme.2025.15439.2961

**Keywords**

*Numerical modeling*

*Finite element method*

*Factor of safety*

**Abstract**

Slope stability is critical for infrastructure safety, particularly in seismically active regions. This work evaluates the stability of a slope along the Baroti-Reyur road in Himachal Pradesh, located in Zone 5, using a novel combination of Limit Equilibrium Methods (LEMs) and Finite Element Methods (FEMs). The analysis examines natural slope conditions and the impact of sustainable mitigation measures, including retaining structures and bioengineering techniques, under the static and dynamic conditions. The soil model incorporated a modulus of elasticity (E) of 90,000 kN/m², and a poisson's ratio (v) of 0.3 to reflect realistic slope-soil-structure interactions. Retaining structures such as gravity, cantilever, and gabion walls (4 m, 6 m, and 5 m high) were constructed using M30 RCC and Fe500 steel. Bioengineering measures featured deep-rooted grasses like Vetiver and Broom grass to improve soil cohesion (c), shrubs like Lantana camara for surface stability, and trees like Albizia lebbeck to reinforce deeper soil layers. These vegetation-based interventions enhanced slope resilience, while promoting ecological restoration. Theoretical LEM analysis revealed marginal stability, with static FOS values of 1.1 and pseudo-static FOS of 1.05. GEO5 pseudo-static analysis indicated critically low FOS value of 0.88 for dynamic saturated conditions, improving to 2.01 with retaining structures. FEM analysis using PLAXIS 2D provided more detailed insights, capturing complex soil-structure interactions with a static FOS of 1.028 and dynamic FOS of 0.994. By combining FEM with sustainable mitigation strategies, this work offers a framework for resilient slope stabilization, ensuring safety, while promoting environmental sustainability in seismically active regions.

## 1. Introduction

Landslides, whether caused by human activities or natural factors, pose significant risks to engineering projects and communities, particularly in steep terrains. These events disrupt ecosystems, and often lead to substantial loss of life and property. Himachal Pradesh, with its rugged topography and heavy monsoon rainfall, is highly susceptible to landslides, especially during the rainy season; contributing factors include urbanization, climatic changes, and intense precipitation, which amplify the risk and extent of damage annually. This work investigates the stability of the slope impacting the Baroti-Reyur road using both the LEM through GEO5 software and the FEM using PLAXIS 2D. The Baroti-Reyur road, a critical 7 km-long village route under HP PWD, division Dharampur, is the sole lifeline for approximately 7,000 residents in the Banal, Sarskan, and Langehar Gram, panchayats of Mandi district. Frequent landslide-induced blockages of this road, not only hinder transportation, but also disrupt utilities such as electricity and water supply, severely affecting the region's daily life and economic activities. effective mitigation strategies are urgently required to reduce the impact of these landslides on infrastructure and local communities. To address the pressing issues in this region; this work evaluates the slope stability using both the LEM and FEM approaches. GEO5 is employed to analyze pseudo-static conditions and failure

*Corresponding author: sahilthakur94180@gmail.com (S. Thakur)*

surfaces, while PLAXIS 2D provides detailed FEM-based analysis, including stress distribution and deformation under both static and seismic conditions. Previous studies have demonstrated the robustness of FEM and LEM in slope stability analysis, with each method offering distinct advantages. FEM, as highlighted in [1], is particularly effective in identifying critical slip surfaces, stress distributions, and deformation patterns, making it suitable for complex geotechnical conditions, especially under seismic loading. In contrast, LEM, as discussed in [2], provides a straightforward, computationally efficient approach for determining FOS and assessing overall stability based on pre-defined failure surfaces. The complementary use of FEM and LEM has been emphasized in multiple studies, particularly in regions prone to seismic activities, where their combined application enhances accuracy by addressing both stress-strain behavior and limit equilibrium conditions. Recent research on slope stability in seismic regions has provided additional insights relevant to this work, uencing failure mechanisms. [4] explored the role of soil-structure interaction in landslide-prone Himalayan terrains, highlighting FEM's ability to model progressive failure mechanisms. [5] analyzed slope stability using numerical methods, demonstrating the role of advanced computational techniques in geotechnical analysis. These recent studies align with the findings of this research work, reinforcing the significance of integrating FEM and LEM for comprehensive stability evaluations. Research specific to Himalayan slopes has also informed this work. [6] reviewed slope stability challenges and mitigation measures in the Lesser Himalayan region, providing insights into geotechnical complexities. [7] analyzed Himalayan slopes using GEO5, integrating advanced anchoring techniques to enhance stability under seismic loading. [8] employed numerical methods for evaluating cave stability, demonstrating the adaptability of FEM to complex geological conditions, while [9] conducted comparative stability studies using GEO5 and PLAXIS 2D, highlighting their reliability for modeling varying geological conditions. [10] explored fractured rock slopes using both FEM and LEM, offering valuable perspectives on integrating these methods for enhanced accuracy. Bioengineering has emerged as a sustainable approach to slope stabilization, particularly in the seismic zone, 5 region of Mandi, Himachal Pradesh. The effectiveness of vegetation-based stabilization techniques has been demonstrated in multiple studies. [11] conducted numerical simulations to assess the contribution of bioengineering techniques to slope stability, emphasizing their role in improving soil cohesion and reducing erosion. [12] investigated bioengineered slopes in Thailand, showing significant stability improvements through vegetation reinforcement. More recently, [13] presented field-based evidence on the effectiveness of root-reinforced slopes under seismic conditions, providing empirical validation for bioengineering measures. [14] conducted a case study in Kangra, Himachal Pradesh, showcasing the effectiveness of bioengineering for landslide disaster risk reduction, while [15] integrated geophysical, geochemical, and geotechnical approaches to develop bioengineering mitigation strategies, emphasizing the importance of multi-disciplinary methods in addressing landslide stability challenges. Additionally, new studies have expanded knowledge on slope stability and mitigation strategies. [16] performed a comparative analysis of slope stability using Slide and PLAXIS 2D software, providing insights into their application in varying geological conditions. [17] examined the stability of a pump house building and water storage tank slope at Narkanda, India, reinforcing the importance of advanced numerical modeling techniques. [18] analyzed deep-seated landslides in Ethiopia using both LEM and FEM, showcasing their application in different geotechnical contexts. [19] investigated uncertainties in slope stability assessment, emphasizing the role of probabilistic methods in geotechnical engineering. [20] explored IoT applications for slope monitoring in open-cast mines, demonstrating technological advancements in real-time geotechnical monitoring. Mitigation measures such as reinforced retaining structures (RCC cantilever and PCC gravity walls), stepped gabion walls, and bioengineering techniques are proposed to enhance slope stability and sustainability. Bioengineering, particularly vegetation-based stabilization, adds a layer of ecological resilience, while addressing long-term soil reinforcement. The combined use of GEO5 and PLAXIS 2D provides a comprehensive assessment of slope stability and reinforces the significance of integrating analytical and numerical methods. By incorporating recent research and highlighting the distinct roles of FEM and LEM, this work contributes to the development of sustainable mitigation strategies in high-risk seismic zones, aligning with modern infrastructure safety standards.

## 2. Studied Area

The studied area, located on Baroti-Reyur road, lies in a landslide-prone region of the Dharampur division in Mandi district, Himachal Pradesh, with geographic coordinates of latitude 31° 46' 56" N and longitude 76° 45' 23" E. The landslide-affected stretch spans from Km 5/120 to 5/210, as shown in the location map in Figure 1. The Baroti-Reyur road originates from National Highway (NH-03) at Baroti village, traverses hilly terrain, and terminates at NH-03 at Chalal, passing through loops with steep gradients. This road has an existing carriageway of 3.05 m with a 5 m roadway. This route passes through hilly terrain that is highly prone to landslides. The residents of connected villages are cut off from the main streams for several months during the rainy season due to road damage and massive landslides. The landslide hazard profile of landslide-prone areas is also shown on the landslide hazard map of Himachal Pradesh, which indicates that the area lies in high hazard (Figure 3). The portion of the road in Km 5/120 to 5/210 is highly prone to landslides. This landslide-prone area is situated on Baroti-Reyur road, leading towards NH-3, having a length of 7.000 Km. At RD 5/120 to 5/210, the slope is steep with an inclination raging up to 60° with a height of about 120 m above the road and 30 m below the road level having a base width of 90 m along the road. The approximate area of the landslide at RD 5/120 to 5/210 is about 12000 m². The landslides at RD 5/120 to 5/210 are complex involving failure of silty sandy clayey soil mixed with fractured sandy rock with debris fall/slide. The slides consist of debris/rockslide/fall at the location, as can be observed in Figure 4. Intense rainfall is the primary factor that triggers the occurrence of landslides, land subsidence, and improper drainage, which caused the seepage of stormwater through pervious soil mixed with fractured rock strata, resulting in subsidence and soil/rockslide. The landslide initiated due to the seepage of surface water into impervious strata containing silty sandy clayey soil which resulted in subsidence and sliding causing slope instability. The major landslide initiated during the recent monsoon and as such, there is no historical background of the landslide. The landslide evolved due to the instability of relatively impervious strata containing silty sandy clayey soil mixed with fractured sandy rock on the slope caused by the saturation due to the seepage of heavy rainwater. The landslide occurred during the recent monsoon and had no recurrence history. At RD 5/120 to 5/210, the approximate area of the landslide is about 12000 m² over a length of more than 150 m. The soil strata of the landslide site at Km 5/120 to 5/210 consist of mainly silty clay mixed with fragmented boulders, as shown in Figure 6.

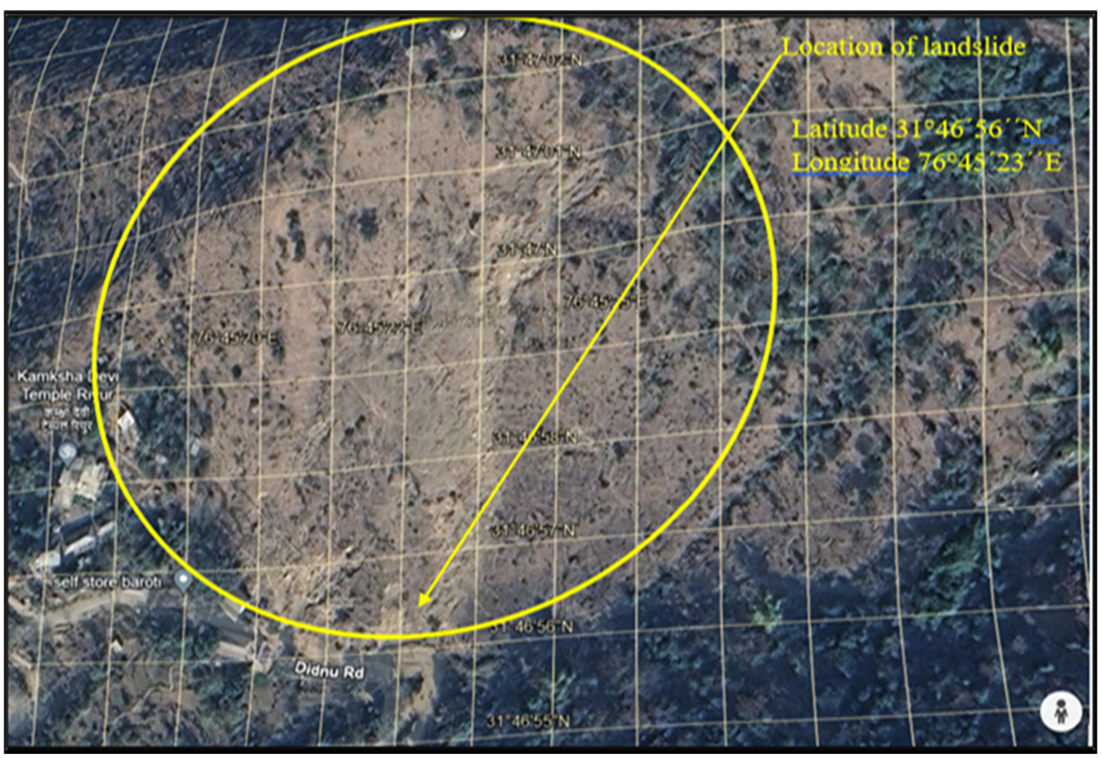


**Figure 1. Location map of landslide-prone area (Source: Google maps).**

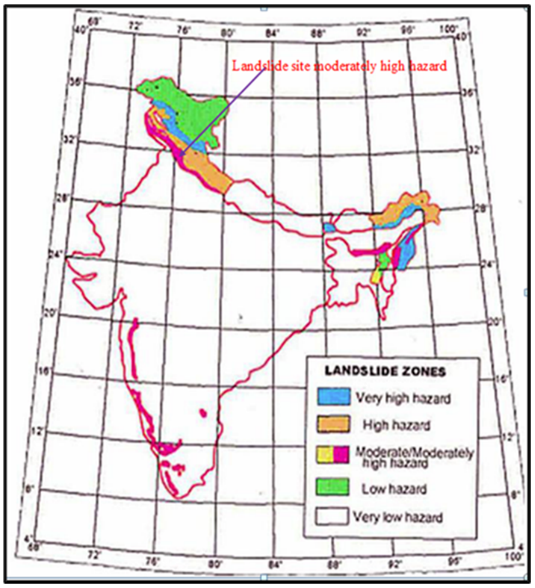


**Figure 2. Hazard profile zonation on map of India**

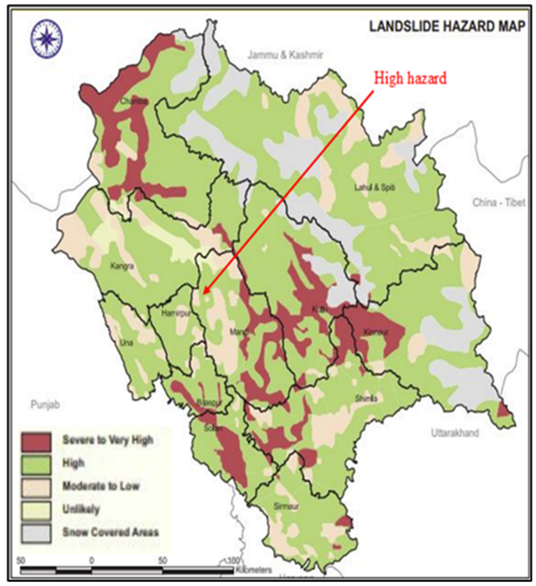


**Figure 3. Hazard profile zonation on map of H.P**

The soil cover mainly consists of silty clay, mixed with fragmented boulders in a complex manner throughout the slope. Improper drainage of the slope leads to the saturation of the weak soil during the rainy season, which decreases the soil's shear strength ($\tau_f$), thereby destabilizing the slope. The primary cause of the landslide is the subsidence of silty and clayey soil on the slope, which occurs due to saturation from stormwater. The extent of the damage caused to the retaining wall and water supply pipes by the landslide is shown in Figure 4 and Figure 5. The drainage of stormwater is not proper, thus making the slope unstable, which resulted in the failure of silty clayey soil mixed with sandstone boulders (Figure 6). Soil samples taken from the landslide area reveal that the soil consists of a silty clay composition, with high compressibility (CH-MH) with medium to hard sandstone. The studied area of Dharampur division is marked by geological features containing mountainous terrain mainly consisting of syncline formations with river sedimentary deposits. These formations were subsequently subjected to folding and thrusting resulting in the formation of hills containing ridges and valleys. The formations mainly consist of Dagshai and Subathu, mainly composed of reddish/greyish Beas shale, mudstone, siltstone, sandstone, and boulderous embedment in alternating layers in a complex manner.

**Figure 4. Comprehensive view of landslide**

**Figure 5. Cracked retaining wall due to landslide**

The rock formations are highly fractured along multiple planes, and often get easily eroded due to various atmospheric agents such as rain, alternate heating, and cooling cycles. The stormwater saturates the poor soil on the steep slopes causing frequent failure resulting in landslides. The dimensions of the landslide indicate 120 m high; and 90 m long slide along the road covering an area of about 12,000 m² with nearly 60,000 cubic meters of total volume at RD 5/120 to 5/210. The scarp of the landslides shows sliding/subsidence at the crown. The crown of the slide is elongated with subsidence and sliding resulting due to seepage of stormwater over the slope. The head of the slides consists of subsidence failure involving soil/rock debris fall/flow. The toe of the slide consists of soil/rock debris deposited along and below the road at the base. The foot of the landslides consists of strata covered with debris of the slides from above. The rupture surface is translational/rotational with complex soil/rock mass subsidence/sliding on the slope. A comprehensive mapping of the landslide site was performed, which involved preparing a contour map of the affected area, and a geological map. The geotechnical investigation of the landslide site was performed by gathering soil specimens from the poor soil on the slope. The soil strata of the landslide site at Km 5/120 to 5/210 consists of mainly silty clayey soil mixed with fragmented sandy rock boulders embedded in between as shown in Figure 7. The soil cover mainly consists of silty clay existing at the top having thickness 2 – 4 m with mixed medium sandstone in a complex manner. The slope is not properly drained which results in the saturation of poor soil on slope during the rainy season reducing the shear strength ($\tau_f$) of the soil thus making the slope unstable. The softening of silty clayey soil due to saturation by stormwater is the main cause of occurrence of landslides.

**Figure 6. Damage caused to water supply pipes**

**Figure 7. Collection of soil samples at landslide**

## 3. Methodology

The integration of PLAXIS 2D and GEO5 offers a robust framework for geotechnical analysis by effectively leveraging the complementary strengths of the FEM and the LEM. PLAXIS 2D employs FEM to perform dynamic analyses that incorporate seismic parameters, such as peak ground acceleration (PGA), providing detailed insights into stress-strain behavior, soil-structure interaction, and deformation, while accommodating complex geometries and boundary conditions. Despite its high accuracy and versatility, FEM is resource-intensive, requiring significant computational power, advanced expertise, and higher costs. On the other hand, GEO5 utilizes LEM to conduct pseudo-static analyses aimed at determining the FOS under seismic conditions. This method, based on simplified assumptions of rigid body movement, is computationally efficient, cost-effective, and ideal for preliminary stability assessments, although it offers limited insights into stress distribution, deformation, and dynamic behavior. LEM assumes slope failure along a pre-defined or assumed slip surface, typically circular or planar, which may not represent the actual failure mechanism. PLAXIS 2D utilizes the FEM for slope stability analysis, employing a plane strain model, where displacements and strains in the out-of-plane direction are assumed to be zero. In contrast, GEO5 primarily uses the LEM for slope stability analysis, evaluating the stability of slopes by analyzing potential failure surfaces and calculating the FOS based on equilibrium conditions. By combining the computational efficiency and simplicity of GEO5 for initial evaluations with the precision and depth of PLAXIS 2D for detailed analyses, this dual approach ensures comprehensive and reliable geotechnical assessments, particularly in seismic conditions. Furthermore, the integration of advanced numerical methods with sustainable strategies enhances the approach's applicability to real-world challenges. Bioengineering techniques were used to evaluate the impact of various vegetation types on improving FOS under seismic conditions, including vetiver grass (chrysopogon zizanioides) for its deep-rooted soil cohesion (c) properties and resistance to shallow landslides ([21]), Lantana camara for reducing surface erosion and slope stabilization ([22]), broom grass (thysanolaena maxima) for erosion control in hilly terrains, and Albizia lebbeck (Siris) for providing deep anchoring and nitrogen fixation, which contribute to long-term slope reinforcement ([23]; [24]). Retaining structures integrated with vegetation were employed as a mitigation strategy to demonstrate their combined effectiveness in addressing seismic vulnerabilities. This comprehensive approach addresses the unique challenges of slope stability in the seismically active zone 5 of Himachal Pradesh, combining advanced numerical methods with sustainable slope stabilization strategies to deliver reliable and resilient solutions.

### 3.1. Soil sampling

The soil sampling process was conducted meticulously to ensure the collection of representative samples from critical sections of the slope prone to failure. Sampling locations were chosen based on observations of silty clayey soils, zones saturated by seeping water, and areas with visible evidence of instability. Soil samples were obtained from the most critical sections of the slope, which exhibited significant clayey soil content, fractured Beas shale, and other poor-quality soils contributing to slope instability. Sampling points were distributed along the landslide site from RD 5/120 to RD 5/210, targeting zones, where subsurface conditions and seepage were deemed to have the greatest impact on slope failure mechanisms. Samples were collected from varying depths to capture a comprehensive profile of subsurface conditions, ranging from surface layers beneath loose debris to bedrock or hard strata, with depths varying from 0.6 m to 4.2 m to encompass loose sandy silts, clayey silts, and fractured rock layers. Core cutters and sampling tubes were used for undisturbed soil sampling, ensuring minimal disturbance to the natural structure and moisture content of the soil. Sampling points were systematically spaced across the site to provide a spatial distribution of samples and cover varying lithological conditions. Samples were carefully sealed and transported to the laboratory to retain their in-situ characteristics. Since standard penetration tests (SPT) were impractical due to fractured rock and debris, Dynamic Cone Penetration Tests (DCPT) were conducted following IS 4968-1 [25], with measurements performed at critical sections. DCPT values (Ncd) at depths from 0.6 m to 4.2 m ranged from 10 to 40, as summarized in Table 1. These values were converted into equivalent SPT values as per IS 4968-1 guidelines, yielding an average N = 20, used for bearing capacity and settlement assessments. The allowable bearing capacity (qu) was computed using IS 8009-1 [26] and IS 1904 [27], resulting in qu = 19.8 t/m² based on a permissible settlement of 50 mm. Borehole logs from RD 5/120 to RD 5/210 revealed a layered subsurface profile: 0–2.4 m of loose sandy silty clay with sandstone boulders, 2.4–3.6 m of medium-dense silty clay with fractured sandy rock, and below 3.6 m of dense silty clay with medium-fractured sandy rock. The physical and mechanical properties of the soil were determined following IS 2720 series codes, including field density (IS 2720-2 [28]) at 1.75 g/cm³ (dry), specific gravity (IS 2720-3 [29]) at an average Gs = 2.65, and Atterberg limits (IS 2720-5 [30]) with a liquid limit of 51.6% and a plastic limit of 42.2%. Statistical analysis of the soil parameters revealed minimal variation, confirming uniformity across the critical sections. Shear strength ($\tau_f$) parameters determined using consolidated undrained triaxial tests (CU tests) in both dry and saturated conditions (IS 2720-11 [31]) showed cohesion (c) of 30 kN/m², angle of internal friction (Ø°) of 30°, unit weight ($\gamma$) of 17.15 kN/m³, and saturated unit weight ($\gamma_{sat}$) of 18.15 kN/m³ as shown in Table 2. The derived soil properties were incorporated into slope stability analyses using GEO5 2D, and input parameters were validated against field observations and laboratory results, forming a reliable foundation for evaluating slope stability and designing mitigation measures.

**Table 1. DCPT values from dynamic cone penetration test.**

| Depth (m) | DCPT value, Ncd |
|---|---|
| 0.60 | 10 |
| 1.20 | 14 |
| 1.80 | 17 |
| 2.40 | 20 |
| 3 | 27 |
| 3.6 | 34 |
| 4.2 | 40 |

**Table 2. Soil parameters.**

| Properties | Soil |
|---|---|
| Cohesion (c) | 30.5 kN/m$^2$ |
| Angle of internal friction (Ø°) | 30° |
| Unit weight ($\gamma$) | 17.15 kN/m$^3$ |
| Saturated unit weight ($\gamma_{sat}$) | 18.15 kN/m$^3$ |

The slope consists of fractured sandy rock boulders mixed with soil, without distinct intact rock layers, making it unnecessary to evaluate rock parameters. Samples of rock and relevant field data were collected to classify the rock based on various characteristics. The Uniaxial Compressive Strength (UCS) of the rock samples was measured at 25.5 MPa, corresponding to a rating of 4. The Rock Quality Designation (RQD) for the rock samples was less than 28%, resulting in a rating of 8. The spacing between discontinuities ranged from 50 to 200 mm, leading to a rating of 8, while the discontinuities had less than 5 mm of condition with severely weathered surfaces, contributing a rating of 10. A rating adjustment of -25 was applied due to the fair condition of discontinuity orientation. Groundwater conditions were damp, providing a rating of 10. The total rating for the rock samples was calculated as 4 + 8 + 8 + 10 + 10 - 25 = 15, classifying the rock as class V, indicating a very poor-quality rock. Adjustment factors for the slope, including parallelism of the slope, discontinuity F1 (very unfavorable), dip of discontinuity F2, and slope inclination F3, were considered in the Slope Mass Rating (SMR) calculation. These adjustments were F1 = 0.15, F2 = 1, and F3 = -25, with an additional adjustment for excavation (F4) of +10. The final SMR was calculated as SMR = RMR + (F1 × F2 × F3) + F4 = 15 + (0.15 × 1 × -25) + 10 = 21.25, placing the slope in class IV, indicating instability and the need for significant corrective action. Based on the rock mass rating, the cohesion (c) of the rock mass is under 100 kPa, and the friction angle (Ø°) is below 15°. Slope stability analysis, conducted using the soil parameters outlined in Table 2 and software such as GE05 and PLAXIS 2D, revealed that the slope becomes stable after implementing suitable mitigation measures at the landslide site. However, the landslide site is fresh, with no present monitoring or real-time data available.

### 3.2. Bioengineering

Bioengineering has been implemented as a key approach to enhance slope stability in the highly seismic zone, 5 regions of Mandi, Himachal Pradesh, specifically for the stabilization of the Baroti-Reyur road slope. This method leverages vegetation to improve soil cohesion, reduce surface erosion, and mitigate landslide risks, with plant species carefully selected for their adaptability to the local environment, rapid establishment, and proven mechanical stabilization properties [22], [24]. The vegetation utilized included deep-rooted perennial grasses like Vetiver (Chrysopogon zizanioides), which enhances soil cohesion and resistance to shallow slips with roots growing up to 3–4 meters, and Broom grass (Thysanolaena maxima), whose dense root mats effectively control erosion in hilly terrains [21]. Shrubs such as Lantana camara and Artemisia vulgaris were incorporated to provide surface protection and improve soil cohesion through their fibrous root systems. Trees including Bauhinia variegata (Kachnar) and Albizia lebbeck (Siris) were strategically planted for reinforcing deeper soil layers and improving slope stability, with Albizia also supporting nitrogen fixation to enhance soil fertility [23], [22]. Mechanically, these species contributed to slope stabilization by increasing soil cohesion through deep and fibrous roots, minimizing direct rainfall impact with dense ground cover, and acting as natural anchors to counter seismic forces [24]. Specific bioengineering techniques included planting Vetiver grass in contour rows for erosion control, establishing Lantana camara on slope edges to stabilize areas prone to shallow landslides, and using Albizia lebbeck alongside retaining structures to anchor deeper soil layers [21]. The region's steep terrain, high monsoonal rainfall, and seismic activity made these vegetation-based measures particularly suitable, with native plant species ensuring high survival rates, ecological restoration, and reduced maintenance costs [32]. An assessment of long-term performance under prolonged wet conditions and seismic shaking is essential to determine the resilience of bioengineering measures. Prolonged wet conditions can reduce soil shear strength, leading to pore water pressure buildup and potential slope failure. The saturation of soil may weaken root anchorage and diminish the stabilizing effects of root reinforcement, as waterlogged conditions often lead to reduced friction between roots and soil particles. On the other hand, seismic events induce dynamic loading that tests the mechanical stability of root-soil composites. During such events, root networks may help dissipate seismic energy by increasing the ductility of the soil mass and reducing surface deformations, although excessive shaking could strain or even rupture roots, compromising their stabilizing effect. Studies from similar landslide-prone regions suggest that vegetation plays a critical role in stabilizing slopes. Research shows that Vetiver and Broom grass can maintain root strength even under high moisture content, effectively stabilizing slopes during heavy monsoons [21], [22]. However, continuous monitoring of root reinforcement under prolonged saturation is necessary, as excess moisture may weaken soil-root interactions over time. In earthquake-prone areas like Japan, Asada and Minagawa [33] highlight that vegetation-based stabilization has demonstrated promising results in mitigating shallow landslides. They emphasize that different types of vegetation can significantly impact slope stability, though seismic shaking may still induce failures in deeper soil layers if not supplemented with structural reinforcements. Integrating these bioengineering methods with structural interventions like gabion walls and RCC retaining structures provided a holistic solution for landslide risk mitigation. The successful stabilization of the slope not only ensured the safety of infrastructure but also promoted ecological balance and sustainable development in this environmentally sensitive area. Future studies should focus on long-term monitoring of bioengineered slopes using inclinometers and root strength assessments to evaluate performance under extreme climatic and seismic conditions. Incorporating findings from case studies in similar terrains would further validate the effectiveness of these measures and provide insights for optimizing their application in high-risk zones [24], [32].

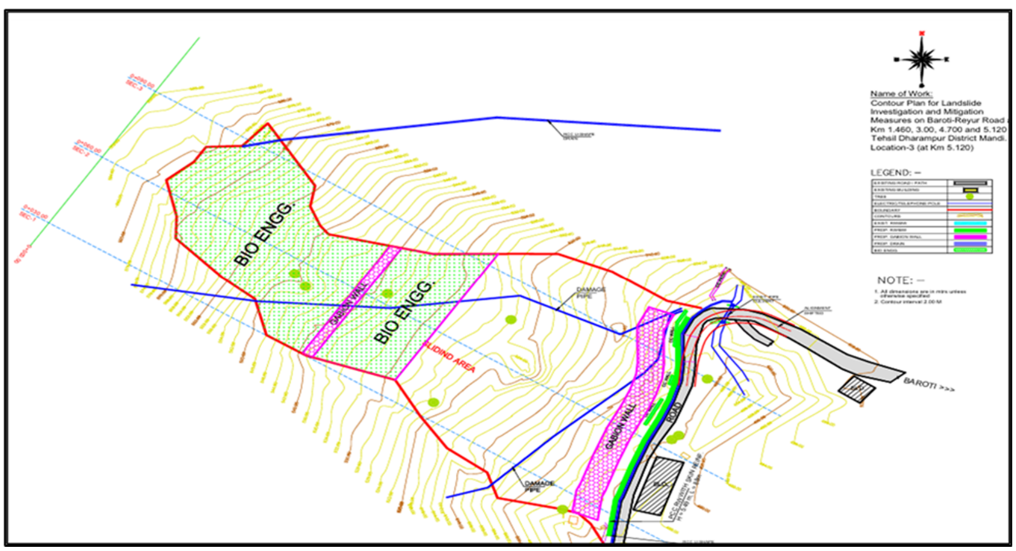


**Figure 8. Contour map showing mitigation measures for landslide.**

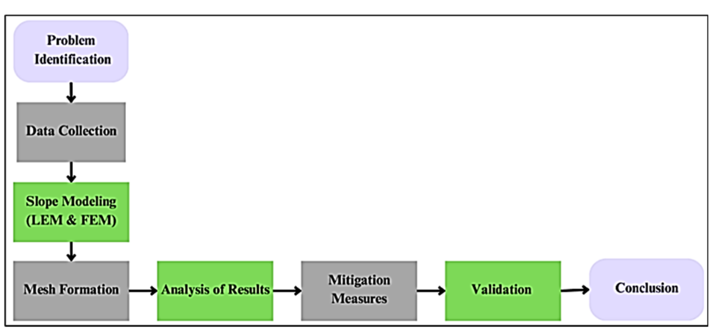


**Figure 9. Flow diagram.**

### 3.3. Theoretical analysis for FOS without mitigation measures

**FOS calculation:**

The FOS is calculated using the equation:

$FOS = (CA + (W \cos \Psi_p - U - V \sin \Psi_p) \tan \Phi)/(W \sin \Psi_p + V \cos \Psi_p)$

where, A is the area of the wedge

$A = (H + b \tan \Psi_s - Z) \text{cosec } \Psi_p$

In Figure 10, the slope height (H), tension crack depth (Z), and the distance (B) from the crest are shown, along with other parameters such as Ψs for the slope above the crest and Ψp for the wedge slope angle. The depth of water in the tension crack is $Z_w$, and Table 3 provides values for analysis, including average values for cohesion (c), friction angle ($Ø^{\circ}$), and unit weight (γ) based on Table 2. The forces acting on the sliding plane and in the tension crack, represented by U and V.

Calculation of forces:

The water force U acting on the sliding plane is given by:

$U = ½ \gamma_w Z_w (H + b \tan \Psi_s - Z) \text{cosec } \Psi_p$

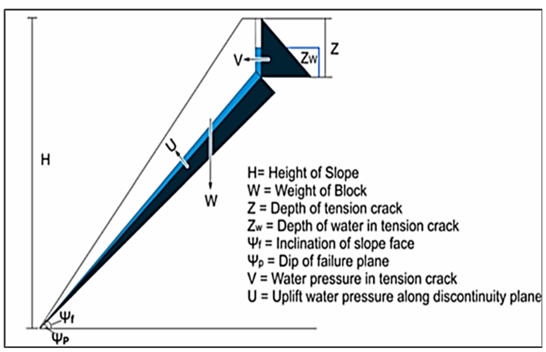


**Figure 10. Plane Wedge Failure [34].**

And the force V within the tension crack is given by:

$V = ½ \gamma_w Z_w^2$

Where $\gamma_w$ is the unit weight of water (10 kN/m³), and W is the weight of the sliding block, calculated as:

$W = \gamma_r [(1 - \cot \Psi_f \tan \Psi_p) (BH + ½) + ½ (\tan \Psi_s - \tan \Psi_p)]$

where $\gamma_r$ (unit weight of rock) = 24 kN/m³.

Critical tension, crack depth, and position:

For a dry slope, the critical depth $Z_c$ of the tension crack is calculated by:

$Z_c/H = 1 - \sqrt{(\cot \Psi_f \tan \Psi_p)}$

And its position $B_c$ behind the crest is given by:

$B_c/H = \sqrt{(\cot \Psi_f \cot \Psi_p)} - \cot \Psi_f$

Using $\cot \Psi_f = 0.9$ and $\cot \Psi_p = 2.05$, we find:

$B_c = 10.54$ m, $Z_c = 7.76$ m

Area calculation:

The area A is determined as:

$A = (H + b \tan \Psi_s - Z) \text{cosec } \Psi_p = 47.532$ m²

**Table 3. Parameters for LEM.**

| Parameter | Units |
|---|---|
| Height | 23 m |
| $\Psi_f$ | 48° |
| $\Psi_p$ | 26° |
| $\Psi_s$ | 28° |
| Area | 47.532 m² |
| W | 6525.398 kN |
| Cos $\Psi_p$ | 0.899° |
| Sin$\Psi_p$ | 0.438° |
| U | 1844.234 kN |
| V | 301.088 kN |
| tan Φ | 0.577° |

Factors of safety for different conditions:

- **Fully filled tension crack:**

If the tension crack is completely filled with water, the FOS is:

FOS = 1.1

- **Partially filled tension crack (¾ depth):**

With $Z_w = 5.82$ m, the values of U and V are:

U = 1383.175 kN, V = 169.362 kN

The resulting FOS is:

FOS = 1.327

- **Drained slope (no water in tension crack):**

When $Z_w = 0$ (no water), and U = 0, V = 0, the FOS is:

FOS = 1.692

- **Reduced cohesion (c) due to vibrations:**

For a drained slope with cohesion (c) reduced to zero, the FOS drops from 1.692 to: FOS = 1.185

- **Pseudo-static method:**

The FOS using the pseudo-static method as per [34] is calculated based on the horizontal seismic coefficient $K_h$, determined using the following equation as per [35]:

$K_h = Z \times I \times S_a/2 \times R \times g$

where:

Z = 0.36 (seismic zone factor for zone 5)

I = 1.5 (importance factor for critical infrastructure)

$S_a/g$ = 2.5 (spectral acceleration coefficient for soil type and seismic zone)

R = 3 (response reduction factor for slopes without ductile reinforcement)

Substituting these values:

$K_h = 0.36 \times 1.5 \times 2.5/2 \times 3 \times 1 = 0.23$

The corresponding vertical seismic coefficient is assumed as:

$K_v = 0.67 \times K_h = 0.153$

The selection of these coefficients follows standard guidelines. The horizontal seismic coefficient $K_h$ accounts for the expected ground shaking intensity, influenced by the seismic zone and site conditions. The response reduction factor R reflects the slope's ability to dissipate energy, set conservatively for an unreinforced slope. The importance factor I ensures that critical infrastructure receives a higher safety margin. The vertical seismic coefficient $K_v$, taken as 67% of $K_h$, follows common engineering practice, considering that vertical acceleration effects are significant but generally lower than horizontal effects in seismic loading scenarios.

Using the pseudo-static method in GEO5 with these coefficients, the calculated FOS is:

$FOS = CA + (W (\cos \Psi_p - K_h \sin \Psi_p)) \tan \Phi)/W (\sin \Psi_p + K_h \cos \Psi_p)$

FOS = 1.05

This analysis assumes that the seismic forces act as equivalent static loads without considering time-dependent effects such as amplification, damping, or transient soil behavior. While this method provides a simplified assessment of seismic stability, it does not capture dynamic stress redistribution or soil strain accumulation, which are better represented in fully dynamic analyses such as those conducted in PLAXIS 2D.

## 4. Numerical modeling

To replicate the actual site conditions, the traditional LEM using GE05 and the FEM using PLAXIS 2D were used. The contour map of the studied area was imported into AutoCAD to extract the relevant interface points, which were subsequently used to define the slope interface in GEO5. Soil properties for the slope, as outlined in Table 2, were incorporated into the GEO5 model. In this model, both soil properties and seismic forces were defined to assess the stability of the slope. A series of FOS checks were performed, with the slope considered stable if the FOS exceeded 1.5, indicating that it could withstand the acting forces and loads. Additionally, the critical section was transferred to PLAXIS 2D, where the soil polygon was drawn, and the corresponding soil parameters were input. A fine mesh was used, and dynamic analysis focused on a 1-meter displacement in the x-direction at the slope's base. This displacement accounted for the horizontal shift of 1 meter caused by seismic forces acting on the slope. The total horizontal length of the slope measures 50 meters, while the vertical height from the base to the top is 23 meters. The slope is at an angel of 48° initially. additionally, the road within the slope showing a horizontal span of 5.2 meters, as shown in Figure 11. These dimensions offer a clear understanding of the scale and proportions of the sloped structure.

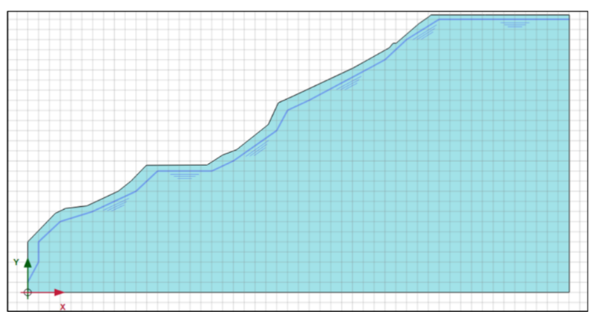

**Figure 11. Slope interface on PLAXIS 2D.**

**Table 4. Parameters adopted for GEO5 and PLAXIS 2D.**

| Parameter | GEO5 | PLAXIS 2D |
|---|---|---|
| Analysis type | Pseudo-static analysis for seismic loading | Dynamic and static analysis |
| FOS calculation | LEM (Bishop's method) | Plane strain model with FEM ( C-phi reduction method) |
| Seismic loading | Pseudo-static approach with seismic parameters | Dynamic loading with time history analysis (PGA values) |
| Mesh type | Not applicable (2D analysis with LEM) | 2D mesh (very fine) |
| Input soil properties | Cohesion (c), friction angle (Ø°), unit weight (γ) from lab tests | Cohesion (c), friction angle (Ø°), unit weight (γ) from lab tests |
| Water table/soil saturation | Fully saturated | Fully saturated |
| Soil behavior model | Mohr-Coulomb | Mohr-Coulomb |

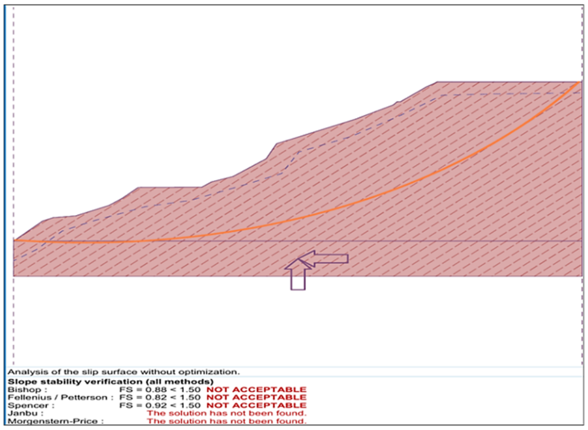


**Figure 12. Pseudo-static FOS = 0.88 without mitigation measures.**

## 4.1. Mesh formation

In PLAXIS 2D, meshing is a crucial step in ensuring accurate numerical simulations by dividing the geometry into smaller finite elements, with the refinement process focusing on improving resolution in critical areas. The process begins with the definition of the model geometry based on the slope's actual dimensions, incorporating layers, boundaries, and reinforcement structures. Material properties, including cohesion, friction angle, and unit weight, are assigned to the respective soil and structural regions. An initial mesh is automatically generated by PLAXIS 2D based on these geometric and material configurations. However, the default mesh often lacks sufficient resolution in zones with high-stress concentrations such as near retaining walls, in areas with complex geometries, including curved or irregular boundaries. To address this, manual refinement is applied, reducing the relative element size to 0.5 and achieving an average element dimension of approximately 1.712 m, balancing computational efficiency with accuracy. A very fine mesh is then selected for the entire model to capture detailed deformation and stress patterns, with particular focus on retaining structures, interfaces between different materials, and slope surfaces prone to failure. The fine mesh selection is justified by its ability to enhance accuracy, especially in capturing gradients in stress and deformation, which are critical for calculating factors such as the FOS, displacement, and stress redistribution. High-resolution meshing is indispensable for modeling localized stress concentrations near retaining walls, soil-reinforcement interfaces, and zones of potential failure surfaces. Additionally, the complex geometry of the slope, with varying inclinations and retaining structures, necessitates a fine mesh to ensure precise representation and minimize numerical errors. In dynamic simulations, a finer mesh improves the resolution of seismic wave propagation and interactions with the slope, providing more reliable results. A mesh sensitivity analysis was conducted to assess the impact of further mesh refinement on the FOS values. The FOS was calculated iteratively through successive mesh refinements, comparing results obtained using different mesh densities. The analysis showed that for a mesh with a relative element size of 0.3, the FOS value increased marginally by 0.78%, while refining further to 0.25 resulted in a change of less than 0.5%. These minimal variations indicated that the selected mesh (relative element size of 0.5) provided sufficient accuracy without excessive computational cost. Displacement convergence was also achieved by monitoring maximum displacement values, with consistent results indicating the reliability of the very fine mesh. Although finer meshes increase computational time, the selected mesh strikes a balance between accuracy and processing requirements, delivering results within a reasonable timeframe. The convergence study confirmed that additional refinement did not significantly alter the FOS or displacement values, validating the adequacy of the chosen mesh. In summary, the use of a very fine mesh, as shown in Figure 13, with a relative element size of 0.5 and average element dimensions of 1.712 m, is justified for capturing critical stress and deformation patterns, accurately modeling complex geometries and dynamic interactions, and ensuring convergence of results through iterative refinement. This approach ensures accuracy, reliability, and robustness in geotechnical analysis while meeting computational efficiency requirements.

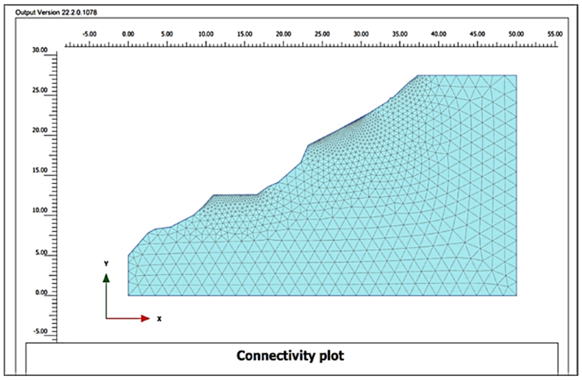

**Figure 13. Mesh formation (very fine).**

### 4.2. Boundary conditions

***$X_{min}$ and $X_{max}$ (left and right boundaries):***

**Static analysis:** The left and right boundaries are horizontally fixed ($u_x$ = 0) to simulate the natural constraints provided by the undisturbed soil mass at the ends of the slope. This assumption is based on the lateral confinement observed in real-world slope systems, where the soil mass at a significant distance from the slope remains relatively undisturbed and provides a lateral boundary effect. vertical movement ($u_y$) is allowed to accommodate settlement due to the influence of gravitational loads. This condition is consistent with empirical recommendations for FEM slope stability modeling [36].

- **Dynamic analysis:** Viscous boundaries are employed to absorb incoming seismic waves and prevent reflections back into the model domain. These boundaries effectively simulate an infinite domain, ensuring the accuracy of dynamic analysis. This approach is well-documented in seismic modeling studies, and is critical to avoid artificially amplifying wave energy within the model [37].

***$Y_{min}$ (Bottom boundary):***

- **Static analysis:** The bottom boundary is fully fixed ($u_x$ = 0 and $u_y$ = 0) to replicate the behavior of the base rock or deeply consolidated soil layers, which are immobile under static loading conditions. This assumption is derived from site-specific geological surveys, indicating the presence of competent rock strata beneath the slope. Fully fixing the bottom boundary ensures stability and prevents unrealistic downward or lateral movement.
- **Dynamic analysis:** A viscous boundary is applied to the bottom in dynamic analysis to absorb seismic energy and prevent artificial wave reflections. The viscous boundary simulates the damping effects of deeper geological layers, consistent with guidelines for dynamic FEM simulations [38].

***$Y_{max}$ (Top boundary):***

- **Static analysis:** The top boundary is left free ($u_x$ and $u_y$ are free) to allow natural deformation under gravitational loads and external forces. This condition reflects the behavior of the ground surface, where no external constraints are typically present. The free boundary ensures realistic settlement and horizontal displacement results.
- **Dynamic analysis:** No boundary condition is applied to the top in dynamic analysis to allow unrestricted surface deformation under seismic loading. This approach accurately replicates real-world seismic effects, where the ground surface is free to respond to seismic forces.

**Table 5. Boundary conditions adopted for FEM analysis.**

| Boundary | Static analysis | Dynamic analysis | Description |
|---|---|---|---|
| Boundary $X_{min}$ (left) | Horizontally fixed ($u_x$ = 0) | Viscous | Mimics lateral constraints of undisturbed soil mass; prevents wave reflections in dynamic analysis. |
| Boundary $X_{max}$ (right) | Horizontally fixed ($u_x$ = 0) | Viscous | Same as above; ensures stability and accurate seismic wave propagation. |
| Boundary $Y_{min}$ (bottom) | Fully fixed ($u_x$ = 0, $u_y$ = 0) | Viscous | Reflects immobility of underlying bedrock; dynamic damping simulates energy absorption by deeper layers. |
| Boundary $Y_{max}$ (top) | Free ($u_x$, $u_y$ free) | None | Allows realistic surface deformation under static loads and seismic effects. |

### 4.3. Static and dynamic analysis

The FOS under seismic loading was calculated as 0.994, as shown in Figure 21, which is below the generally accepted threshold of 1.2 for dynamic safe slope conditions as per [39]. This significant reduction highlights the critical need for stabilization measures, particularly in seismic zone 5 regions, where the risk of earthquake-induced slope failure is highest. Zone 5 represents the highest seismic risk category in India, with maximum expected PGA of 0.36 g (approximately 3.5 m/s²) during major earthquakes as per [35]. The modeled maximum acceleration of 1.33 m/s², though lower than the maximum PGA, reflects realistic earthquake scenarios for the region. An FOS of 0.994 indicates that the slope is highly susceptible to failure during seismic events, rendering it unable to resist the destabilizing forces caused by ground shaking. This poses a significant threat to critical infrastructure including roads, retaining structures, and utility lines. For example, in the case of the Baroti-Reyur road, such instability could result in prolonged road closures, disrupted services, and increased risks to nearby communities. To mitigate these risks, infrastructure design in zone 5 must prioritize robust stabilization measures. Retaining structures such as Reinforced Concrete (RCC) cantilever walls and stepped gabion walls, are essential for counteracting seismic-induced forces and enhancing slope stability. These structures should be designed to withstand both static and dynamic earth pressures. Effective drainage systems are also critical to minimize the buildup of pore water pressure, which can amplify seismic vulnerability. Vegetative stabilization using deep-rooted plants can complement structural reinforcements by improving soil cohesion (c) and reducing the likelihood of seismic-induced landslides, especially in areas where space or cost constraints limit the use of extensive retaining structures. The dynamic analysis, which resets displacement to zero before the dynamic phase, ensures that pre-seismic deformation does not skew results. By retaining stresses and strains from the static phase, the analysis accurately reflects the pre-seismic condition, making the results realistic. The time-history loading, with a maximum acceleration of 1.33 m/s² occurring at 0.1 seconds and a total duration of 10 seconds, aligns with typical earthquake characteristics for zone 5, and demonstrates the slope's inability to maintain stability under such conditions. The required time step was taken as 0.001 sec for the dynamic phase calculation for maximum accuracy of the dynamic analysis. Recommendations for infrastructure design in zone 5 include adhering to stringent seismic design standards, such as those outlined in [35] and [40], to ensure the resilience of critical infrastructure. Furthermore, planning for emergency preparedness including redundancy and alternative routes is essential to maintain community access during post-earthquake recovery periods. The dynamic analysis results underscore the seismic vulnerability of the Baroti-Reyur slope, with an FOS of 0.994 highlighting an urgent need for stabilization measures tailored to the region's seismic risks. By incorporating robust retaining structures, effective drainage systems, and bioengineering techniques, the seismic impacts on slopes can be mitigated, thereby safeguarding critical infrastructure and ensuring long-term safety and resilience against earthquake-induced slope failures. The results shown represent a static FEM analysis using PLAXIS 2D for the initial phase of gravity loading. This phase establishes the initial stress distribution caused by the self-weight of the soil and materials in the model, which is critical for determining stability. The deformed shape of the mesh is scaled up by 50 times for better sisualization. The color contours represent the magnitude of displacement (u), with a maximum value of 0.05112 m occurring at Element 1791, Node 174, as shown in Figure 14. Gravity loading helps analyze the system's stability and stress state before further loading or construction stages, commonly used in slope stability, foundation design, and earthwork assessments.

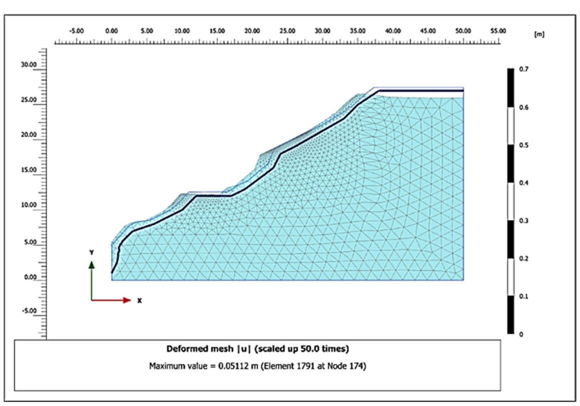


**Figure 14. Initial phase deformed mesh (Static analysis initial phase).**

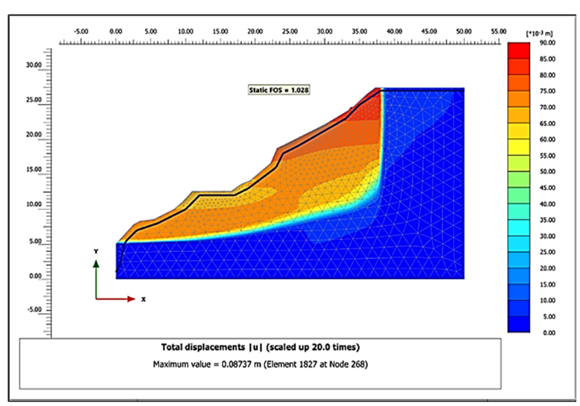


**Figure 15. Total displacement (Static analysis safety phase).**

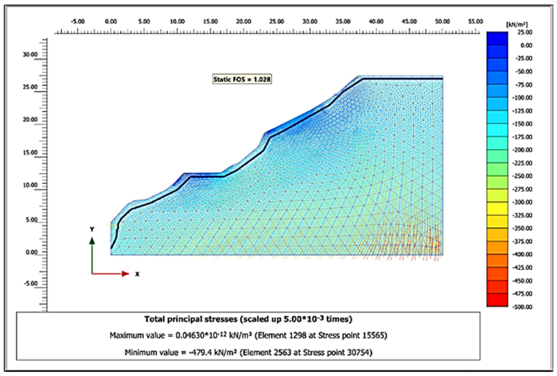


Figure 16. Total principal stresses (Static analysis safety phase)

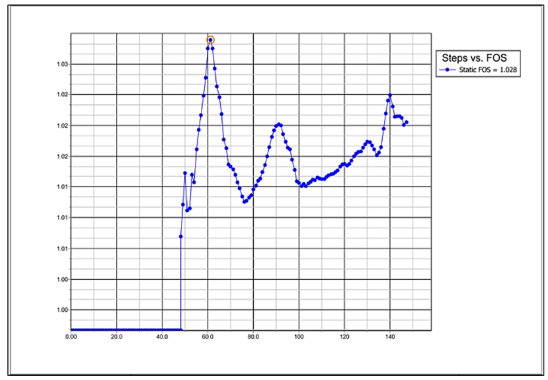


Figure 17. Static FOS = 1.028.

In slope stability analysis, total displacements and total principal stresses are essential for evaluating slope performance and safety. Total displacements indicate soil movement caused by gravity, external loads, or seismic forces, highlighting deformation patterns and potential failure zones. Total principal stresses, comprising maximum and minimum stresses, reveal the internal stress distribution and potential failure planes within the slope. Together, these parameters provide insights into stress-strain behavior, failure mechanisms, and zones of instability. Advanced tools like PLAXIS 2D and GEO5 are often used to analyze these factors and ensure reliable slope designs and mitigation strategies. Principal stresses and total displacements provide detailed insights into material behavior and structural response under static loading conditions. Principal stresses represent the extreme normal stresses acting on specific planes, where shear stress($\tau$) is zero, which are essential for evaluating material stability. In this static analysis, the principal stresses have been scaled by $5.00\times10^{-3}$ for enhanced visualization. The maximum observed principal stress is 0.04630 $\times$ $10^{-12}$, localized at element 1298 and stress point 15565, while the minimum stress is −479.4 kN/m$^2$, indicating significant compressive forces at element 2563 and stress point 30754 as shown in Figure 16. The stress distribution plot highlights regions under tension and compression, crucial for identifying areas susceptible to failure. Similarly, total displacement (u) measures the magnitude of movement from the original position due to applied loads. Displacements were scaled up by a factor of 20 for better visualization, with the highest displacement recorded as 0.08737 m at element 1827 and node 268, as shown in Figure 15. This analysis shows variations in deformation, from negligible in stable regions to significant in vulnerable areas. These results are pivotal for assessing deformation hotspots, stress concentrations, and the need for structural reinforcements or redesign to prevent potential failures under static conditions.

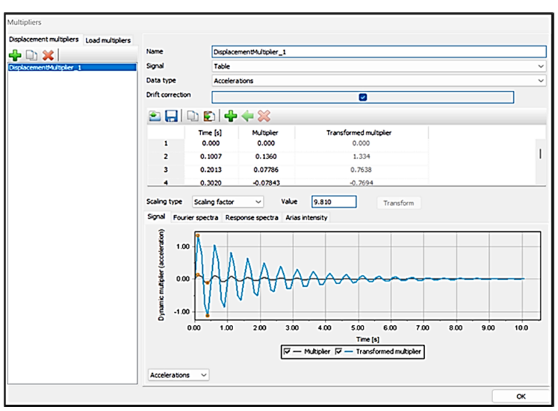


Figure 18. Zone 5 earthquake accelerations (10 sec).

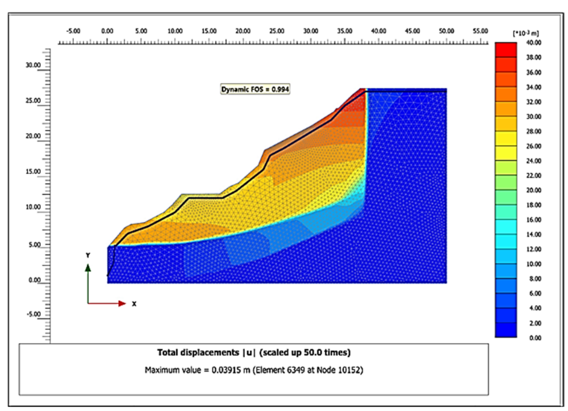


Figure 19. Total displacement (Dynamic analysis safety phase).

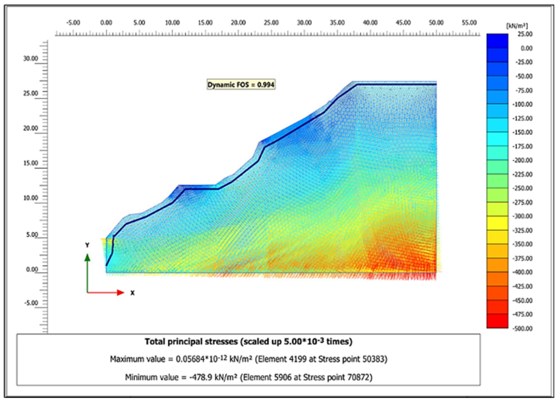


**Figure 20. Total principal stresses (Dynamic analysis safety phase).**

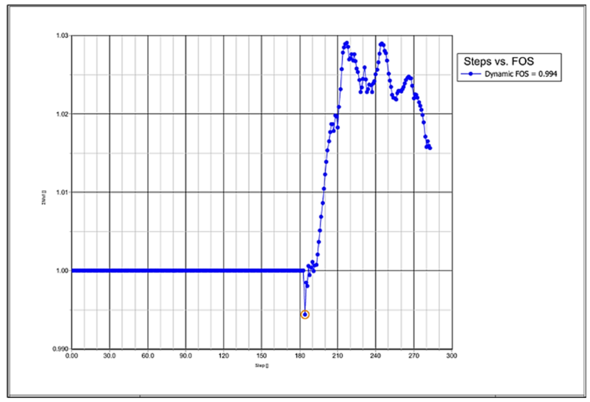


**Figure 21. Dynamic FOS = 0.994.**

Principal stresses and total displacement are critical for analyzing material behavior and structural response under dynamic loads. Principal stresses, representing the maximum and minimum normal stresses on planes where shear stress (τ) is zero, are essential for evaluating material stability. In this analysis, the stresses are scaled by $5.00\times10^{-3}$ to enhance visualization. The maximum principal stress observed is $0.05684\times10^{-12}$ kN/m$^2$, a localized phenomenon at element 4199 and stress point 50383, while the minimum stress, −478.9 kN/m$^2$, indicates dominant compressive forces in specific regions like element 5906 and stress point 70872 as shown in Figure 20. Stress distribution plots reveal tension and compression zones, aiding in identifying potential weak points. Similarly, total displacement (u), the magnitude of the vector sum of displacements in all directions, offers insights into structural deformation. Scaled by a factor of 50 for better visualization, the maximum displacement of 0.03915 m occurs at element 6349 and node 10152 as shown in Figure 19. The displacement pattern highlights deformation hotspots, with values ranging from negligible to maximum, signaling potential instability. These results are crucial for identifying areas requiring structural reinforcement or redesign to prevent failure under dynamic loading.

### 4.4. Mitigation statergies

In studying the unreinforced Baroti-Reyur slope, it's observed that the FOS becomes zero at the failure point, indicating slope instability as the soil enters a plastic state. This failure typically begins at the slope's top, where soil detaches due to tension, causing a slip along the zone of plastic deformation. With an FOS below 1, failure is imminent for the unreinforced slope. However, adding retaining walls significantly improves stability, increasing the FOS and reinforcing the slope. When the slip surface meets the retaining wall, the wall resists the soil movement caused by sliding. This resistance mobilizes passive earth pressure, as the wall pushes into the soil rather than moving away. Without reinforcement, the slope's FOS is 0.88. The angle of friction (δ) between the retaining wall and the soil taken in this study was 0 degrees ($\delta = 0^{\circ}$) as a conservative approach to ensure maximum safety. This is a highly conservative assumption in design of retaining walls because it maximizes the lateral earth pressure acting on the wall. Retaining walls improve this to 2.01, with safety values varying by calculation method: 2.01 by Bishop, 1.92 by Fellenius/Petterson, 2.05 by Spencer, and 2.07 by both Janbu and Morgenstern-Price methods.

The FOS values from various methods using GEO5, as illustrated in Figure 22, are as follows:

a) Bishop: FOS = 2.01, which is above 1.5 (Acceptable)

b) Fellenius/Petterson: FOS = 1.92, exceeding 1.5 (Acceptable)

c) Spencer: FOS = 2.05, greater than 1.5 (Acceptable)

d) Janbu: FOS = 2.07, above 1.5 (Acceptable)

e) Morgenstern-Price: FOS = 2.07, also above 1.5 (Acceptable)

Each method demonstrates an FOS that meets the acceptable safety threshold of 1.5.

**Table 6. Parameters adopted for mitigation.**

| Parameters | Description |
|---|---|
| Type of retaining walls | Gravity, Cantilever, Gabion |
| Height of retaining walls | 4 m, 6 m, 5 m |
| RCC mix and grade of steel | M30, Fe500 |
| Modulus of elasticity (E) | 90000 kN/m$^2$ |
| Poisson's ratio (v) | 0.3 |

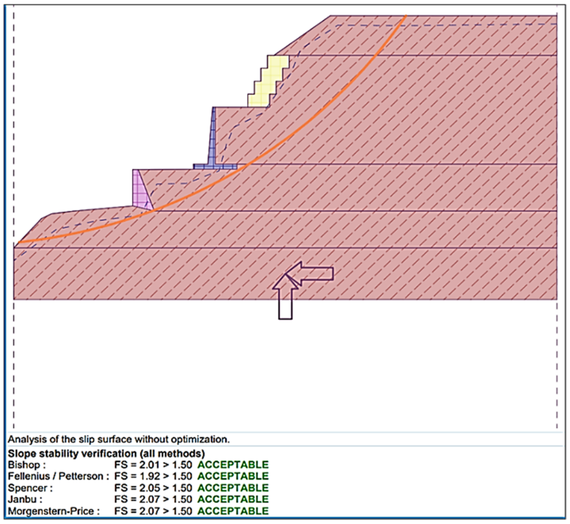


**Figure 22. Pseudo-static FOS = 2.01 with mitigation measures.**

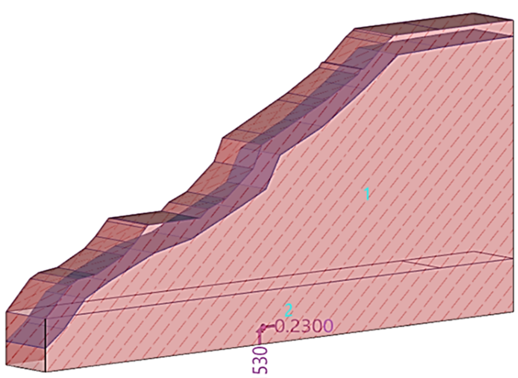


**Figure 23. 3D visualization of the slope without mitigation measures.**

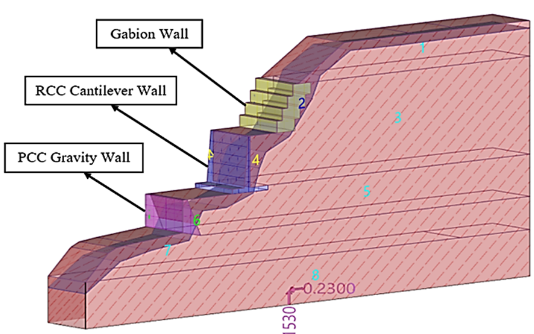


**Figure 24. 3D visualization of the slope with mitigation measures.**

## 5. Results and validation

The slope stability analysis of the Baroti-Reyur landslide in the highly seismic zone 5 region of Himachal Pradesh was conducted using GEO5 and PLAXIS 2D, incorporating both the LEM and FEM. The results revealed that the unreinforced slope was highly unstable, with a pseudo-static FOS of 0.88 (GEO5), as shown in Figure 12 and a dynamic FOS of 0.994 (PLAXIS 2D), as shown in Figure 21, both falling below the safety thresholds of 1.5 and 1.2, respectively. Static analysis in PLAXIS 2D yielded a marginal FOS of 1.028, as shown in Figure 17; further highlighting the need for stabilization measures. Theoretical calculations of static and pseudo-static analyses showed an FOS of 1.1 and 1.05, which aligned closely with the software-generated values, confirming the reliability of the analysis. Upon implementing mitigation measures, particularly retaining walls, the pseudo-static FOS increased significantly to 2.01, exceeding the safety benchmark, and demonstrating the effectiveness of reinforcement techniques in reducing deformation and enhancing stability. These findings emphasize the importance of integrating structural interventions like retaining walls with advanced analysis methods to ensure the safety and stability of slopes in earthquake-prone regions. The validation of the FOS through the LEM using GEO5 and the FEM using PLAXIS 2D was reinforced by field observations and case studies with comparable geological and seismic conditions. Field observations at the landslide site revealed tension cracks, localized subsidence, and seepage zones, which aligned with the low FOS values from the analyses. These physical manifestations of instability indicate that the numerical results accurately represent the real-world behavior of the slope under both static and seismic conditions. Comparisons with observed landslide behavior in similar geological settings further substantiate these findings. Located in zone 5 of Himachal Pradesh, an area prone to frequent seismic activity, the observed failure patterns corroborated the predicted instability under pseudo-static and dynamic conditions. Case studies, such as those on NH-205 [41], reported geological profiles and FOS values consistent with this study's findings, validating the results. In nearby regions with similar soil compositions, including loose sandy silts, clayey silts, and fractured Beas shale, past landslides have exhibited comparable failure mechanisms, including shallow slips, progressive slope failure, and erosion-triggered instability. These similarities reinforce the applicability of the current study's findings to broader geotechnical assessments in seismic-prone mountainous terrain. Although Khanna and Dubey [42] did not report specific FOS values, their comparative assessment of slope stability in the Kullu region under similar seismic conditions emphasized the importance of detailed numerical modeling to capture real-world slope behavior accurately. The seismic loading parameters, such as PGA values, adhere to IS 1893-1 [35] guidelines, further affirming the reliability of the study. By drawing parallels between numerical predictions and observed landslide behaviors, the study underscores the necessity of integrating advanced slope stability analysis with empirical field assessments to develop more effective mitigation strategies.

**Table 7. Results.**

| Analysis method | Software/Approach | Loading condition | FOS | Remarks |
|---|---|---|---|---|
| Pseudo-static analysis | GEO5 | Pseudo-static | 0.88 | Below safe threshold; slope is unstable. |
| Pseudo-static analysis | Theoretical | Pseudo-static | 1.05 | Unstable and vulnerable. |
| Static analysis | Theoretical | Static | 1.1 | Unstable. |
| Static analysis | PLAXIS 2D | Static | 1.028 | Unstable. |
| Dynamic analysis | PLAXIS 2D | Dynamic | 0.994 | Unstable under seismic loading. |
| Mitigation measures (Walls) | GEO5 | Pseudo-static (with walls) | 2.01 | Significantly improves stability; safe slope. |

## 6. Error and limitation analysis

The modeling approach used in this study offers valuable insights into slope stability; however, several limitations and assumptions must be acknowledged to identify potential sources of error in the FOS calculation. First, the analysis assumes soil homogeneity, with uniform soil properties across the modeled slope. In reality, slopes often exhibit variability in soil composition such as differences in cohesion, friction angle, and moisture content at different depths or locations, which can significantly affect stability. Additionally, the Mohr-Coulomb failure criterion employed in both GEO5 and PLAXIS 2D assumes a linear elastic-perfectly plastic material model, which may not fully represent the complex behavior of soils, especially in highly fractured or weathered rock areas common in the studied region. The Mohr-Coulomb model does not account for strain softening, stiffness degradation, or progressive failure mechanisms, which are critical under seismic loading conditions. More advanced constitutive models such as the hardening soil model or modified cam clay could better capture soil behavior under cyclic loading including plasticity effects and strain accumulation. The slope geometry is also simplified in the model, whereas actual slopes often have complex shapes, varying layers, or discontinuities like faults that could influence stability in ways not captured by the analysis. Seismic analysis introduces additional limitations, as the dynamic model incorporates earthquake ground motion parameters based on PGA values for Zone 5, but accurately predicting site-specific seismic ground motion characteristics such as frequency content, duration, and directionality remains challenging. The absence of precise site-specific seismic data may lead to discrepancies between the modeled and actual slope response during seismic events. Additionally, the assumption of constant soil properties under dynamic loading is an oversimplification. In practice, soil strength and stiffness can degrade due to cyclic loading, particularly in loose or saturated soils, potentially causing a reduction in FOS that is not accounted for in the analysis. The Mohr-Coulomb model does not explicitly simulate pore pressure generation and dissipation under cyclic loading, which may influence the stability of saturated soils during seismic events. Bioengineering integration also introduces limitations. The analysis assumes ideal growth conditions for the proposed vegetation species, but factors such as soil fertility, water availability, and climate variations could significantly influence root strength and the overall effectiveness of vegetation in stabilizing slopes. Additionally, the modeling of bioengineering strategies within FEM assumes idealized root reinforcement effects. The actual effectiveness of vegetation, especially in stabilizing steep slopes during seismic events, may vary and is difficult to quantify without extensive field data. Numerical modeling errors present another source of potential inaccuracies. While mesh refinement and sensitivity analyses were conducted to enhance FEM accuracy, numerical errors related to mesh size, boundary conditions, and convergence criteria could still slightly affect the calculated FOS. The choice of boundary conditions in both GEO5 and PLAXIS 2D could also be a source of error, particularly in dynamic analyses, where inaccuracies in boundary representation may alter stress distributions and FOS results. The assumption of rigid bedrock at a predefined depth may not reflect actual site conditions, potentially influencing the stress distribution and failure mechanism. Finally, uncertainties in soil properties contribute to potential errors. The soil properties used in the study, derived from laboratory and field tests, are subject to inherent variability. Factors such as weak layers, seasonal changes, or the effects of soil disturbance could lead to discrepancies in the predicted FOS. Laboratory tests for shear strength, consolidation, and Atterberg limits might not fully represent in-situ conditions, especially in fractured or layered soils. Incorporating probabilistic analyses or Monte Carlo simulations could provide a more comprehensive understanding of uncertainty in soil parameters and their effect on slope stability. In conclusion, while the dual approach of combining FEM and LEM provides a robust framework for slope stability analysis, the assumptions regarding soil homogeneity, seismic loading, and bioengineering integration, along with the limitations of numerical modeling, introduce potential sources of error. The limitations of the Mohr-Coulomb failure criterion in capturing complex soil behavior under seismic loading further emphasize the need for advanced constitutive models to improve the accuracy of stability assessments. One key limitation of the Mohr-Coulomb criterion is its assumption of a linear relationship between shear strength and normal stress, which may not fully represent the non-linear and dynamic behavior of soils during seismic events. This simplification neglects important factors such as strain rate effects, stress path dependency, and cyclic loading responses. These limitations highlight the potential for inaccuracies in predicting failure mechanisms under complex seismic conditions. Therefore, these factors must be carefully considered when interpreting results. Future research should focus on incorporating more sophisticated material models that account for these complexities, as well as probabilistic approaches, to refine slope stability predictions and enhance the reliability of assessments.

## 7. Future directions

Future directions in slope stability research and practice highlight the need for advanced soil behavior models, optimized bioengineering techniques, enhanced numerical modeling, comprehensive field validation, and the integration of climate change considerations. Nonlinear constitutive models, such as the Hardening Soil Model or Modified Cam Clay, can more accurately capture the complex behavior of soils under seismic loading, accounting for plasticity, soil dilation, and strain hardening, particularly in fractured or weathered rock zones common to complex slopes. Incorporating sophisticated soil-structure interaction (SSI) models would enable a more realistic evaluation of how built structures, such as retaining walls or foundations, interact with the slope during seismic events. Additionally, including soil liquefaction analysis in regions with loose or saturated soils is crucial, as liquefaction significantly reduces soil strength and increases the risk of failure under strong seismic shaking. Optimization of bioengineering techniques could involve selecting plant species tailored to site-specific conditions, such as soil type, moisture availability, and seismic vulnerability, alongside conducting long-term studies on root development and seismic resilience. Soil microbial activity could be harnessed to enhance cohesion, with microorganisms promoting soil aggregation and interacting synergistically with plant roots to improve slope stability. Advancements in planting techniques, including geogrid or mesh reinforcement combined with vegetation, and research into optimal spacing and planting patterns, could further enhance soil shear strength in high-seismic zones. Emphasizing native plant varieties adapted to local conditions would promote ecological sustainability, biodiversity, and slope stability, particularly through their ability to resist erosion and increase soil strength during intense rainfall or seismic events. Enhanced numerical modeling techniques, such as transitioning from 2D to 3D finite element analysis (FEA), would allow for more accurate representation of complex slope geometries, soil layers, and discontinuities, improving stress and displacement predictions. Probabilistic modeling approaches, incorporating uncertainties in soil properties, seismic loading, and bioengineering performance, would provide a more comprehensive understanding of risks, while hybrid methods combining FEM and discrete element methods (DEM) could deliver detailed insights into soil failure mechanisms, especially in granular or fractured soils. Field validation and monitoring remain critical, with the installation of sensors like inclinometers, piezometers, and geotechnical accelerometers providing real-time data on soil movement, pore-water pressures, and seismic vibrations to refine numerical models.

Long-term monitoring of slopes under varying climatic and seismic conditions including tracking plant growth and root systems would yield invaluable data to evaluate and enhance bioengineering strategies. The integration of real-world monitoring data with machine learning techniques presents a promising approach for slope stability assessment, enabling the development of predictive models based on historical and real-time data. Machine learning algorithms can analyze large datasets from geotechnical sensors, satellite imagery, and field studies to improve early warning systems, optimize mitigation strategies, and refine numerical models. Finally, integrating climate change models into slope stability studies is essential to address the impacts of shifting rainfall patterns, increased rainfall intensity, and rising temperatures on soil behavior, moisture retention, and plant growth. This integration is particularly significant in regions like Himachal Pradesh, where heavy monsoons and temperature changes exacerbate slope instability. By incorporating machine learning-driven predictive models alongside climate impact assessments, future research can provide more accurate risk assessments and enhance mitigation strategies. By pursuing these directions, slope stability in high-risk seismic zones can be assessed and improved more accurately, ensuring safer, more sustainable infrastructure development in challenging terrains.

## 8. Conclusions

- The study evaluated a slope in Himachal Pradesh, highlighting its vulnerability to instability under both static and seismic conditions, with a specific focus on high-risk seismic zones like zone 5. The findings revealed significant risks to infrastructure and public safety, emphasizing the urgent need for comprehensive slope stability assessments in seismically active regions to mitigate potential hazards.
- Advanced geotechnical analysis was conducted using GEO5 and PLAXIS 2D, incorporating both the LEM and the FEM. The results indicated critical instability under seismic conditions, with GEO5's pseudo-static analysis yielding a FOS of 0.88. Similarly, PLAXIS 2D showed marginal stability, with an FOS of 1.028 under static conditions and 0.994 under seismic loading, demonstrating the severe impact of seismic forces on slope stability.
- The destabilizing effects of seismic activity were evident as inertial stresses reduced the stability of the slope. This emphasizes the importance of accounting for both static and dynamic forces in geotechnical assessments, particularly in earthquake-prone areas. Neglecting seismic effects can lead to an overestimation of slope stability, resulting in a heightened risk of infrastructure failure and public safety concerns.
- To enhance stability, mitigation measures such as retaining walls and bioengineering techniques were employed. Retaining walls significantly improved stability by raising the pseudo-static FOS to 2.01, surpassing the required safety threshold of 1.5, thereby ensuring safety under both static and seismic conditions. This structural intervention played a crucial role in counteracting the destabilizing effects of seismic forces and preventing potential slope failures.
- Bioengineering techniques were integrated as a complementary stabilization measure, utilizing deep-rooted grasses like Vetiver (Chrysopogon zizanioides) and Broom grass (Thysanolaena maxima) to enhance soil cohesion and control surface erosion. Additionally, shrubs such as Lantana camara and Artemisia vulgaris were employed for surface stabilization, while trees like Bauhinia variegata (Kachnar) and Albizia lebbeck (Siris) reinforced deeper soil layers. These plant species were strategically selected for their mechanical stabilization properties, adaptability to local conditions, and ecological benefits.
- The combination of engineered solutions and bioengineering techniques proved highly effective in creating a sustainable, eco-friendly approach to slope stabilization. Vegetation-based methods not only improved soil stability but also contributed to long-term environmental benefits such as reducing maintenance costs, enhancing biodiversity, and promoting ecological restoration. This integrated approach provides a cost-effective and sustainable alternative to conventional geotechnical stabilization methods.
- The study underscores the necessity for engineers to adopt both LEM and FEM approaches for comprehensive slope stability assessments, particularly in seismically active zones like Himachal Pradesh. Structural reinforcements such as retaining walls should be prioritized for critical slopes, while bioengineering techniques can serve as a valuable supplement, reducing long-term maintenance costs and supporting sustainable development initiatives.
- Policymakers should mandate detailed static and dynamic slope stability assessments for infrastructure projects in seismic regions to enhance safety and resilience. Additionally, integrating bioengineering techniques into slope stabilization policies can promote eco-friendly and sustainable geotechnical solutions. Future

research should focus on advanced numerical modeling, real-time monitoring, and large-scale implementation of combined stabilization techniques to improve slope failure predictions and mitigation strategies.

## Acknowledgement

This research complies with the ethical standards of the *Journal of Mining and Environment*. Informed consent was obtained from all participants involved in the study. The authors would like to express their sincere gratitude to all participants for their valuable time and insights. We also acknowledge that no specific funding was provided for this research by any government, corporate, or non-profit organization. Additionally, we extend our appreciation to the editorial board and reviewers of the *Journal of Mining and Environment* for their constructive feedback and support during the publication process.

## References

[1]. Griffiths, D. V., & Lane, P. A. (1999). Slope stability analysis by finite elements. *Geotechnique*, *49*(3), 387-403.

[2]. Hammouri, N. A., Malkawi, A. I. H., & Yamin, M. M. (2008). Stability analysis of slopes using the finite element method and limiting equilibrium approach. *Bulletin of Engineering Geology and the Environment*, *67*, 471-478.

[3]. Santo, S. A., Hossain, A. F., Fariha, A. S., Haque, M. E., & Ansary, M. A. (2024). Assessment of seismic slope stability of Rangamati Hill Tracts, Bangladesh. *Discover Geoscience*, *2*(1), 1.

[4]. Singh, P., & Mittal, S. FINITE ELEMENT SLOPE STABILITY ANALYSES OF A SLOPE IN THE HIMALAYAN REGION OF INDIA CONSIDERING SELF-DRILLING ANCHORS.

[5]. Garo, T., Tesfaye, M., & Karuppannan, S. (2024). Slope stability modeling using limit equilibrium and finite element methods: a case study of the Adama City, Northern Main Ethiopian Rift. *Quaternary Science Advances*, *15*, 100228.

[6]. Jhinkwan, V. S., Chore, H. S., & Kumar, A. (2024). Assessment of Stability of Slopes and Remedial Measures in Lesser Himalayan Region: An Overview. *Indian Geotechnical Journal*, 1-23.

[7]. Arun, K. U., Jisna, P., Simon, R., Mathews, O. A., & Anju, E. M. (2020). A comparison study on stability of Kuranchery slopes using GEO5 and PLAXIS 2D software. *International Journal of Research in Engineering, Science and Management*, *3*(3), 4.

[8]. Alemdag, S., Zeybek, H. I., & Kulekci, G. (2019). Stability evaluation of the Gümüşhane-Akçakale cave by numerical analysis method. *Journal of Mountain Science*, *16*(9), 2150-2158.

[9]. Luc Leroy, M. N., Kenmoe, O. R. M., Tchognia Nkuissi, H. J., Lawou Kouayep, S., Nkenwoum Chebou, G., Chéagé Chamgoué, A., & Mohamadou, I. (2024). Comparative Analysis of the Slope Stability Using Slide and Plaxis 2D Software: A Case Study of Tombel Pozzolan Quarry (South-West Cameroon). *Applied and Environmental Soil Science*, *2024*(1), 8260177.

[10]. Kadakci Koca, T., & Koca, M. Y. (2020). Comparative analyses of finite element and limit-equilibrium methods for heavily fractured rock slopes. *Journal of Earth System Science*, *129*(1), 49.

[11]. Ongpaporn, P., Jotisankasa, A., & Likitlersuang, S. (2022). Geotechnical investigation and stability analysis of bio-engineered slope at Surat Thani Province in Southern Thailand. *Bulletin of Engineering Geology and the Environment*, *81*(3), 84.

[12]. Patial, S., Kumar, V., Sharma, H., Mahajan, A. K., Kumar, P., & Negi, S. (2022). Landslide disaster risk reduction through Bioengineering at Soldha, Kangra, Himachal Pradesh-A case study.

[13]. Patial, S., Kumar, V., Sharma, H., Mahajan, A. K., Kumar, P., Pandey, A. K., & Negi, S. Assessing Landslide Stability: Integrating Geophysical, Geochemical, and Geotechnical Approaches for Bioengineering Mitigation.

[14]. Ray, A., Bharati, A. K., Verma, H., Rai, R., & Singh, T. N. (2023). Numerical study of the utility of bioengineering technique for slope stabilisation. *Geomechanics and Geoengineering*, *18*(4), 253-271.

[15]. Saim, N. M., & Kasa, A. (2023, August). Comparative analysis of slope stability using finite element method (FEM) and limit equilibrium method (LEM). In *2023 IEEE 14th Control and System Graduate Research Colloquium (ICSGRC)* (pp. 224-229). IEEE.

[16]. Luc Leroy, M. N., Kenmoe, O. R. M., Tchognia Nkuissi, H. J., Lawou Kouayep, S., Nkenwoum Chebou, G., Chéagé Chamgoué, A., & Mohamadou, I. (2024). Comparative Analysis of the Slope Stability Using Slide and Plaxis 2D Software: A Case Study of Tombel Pozzolan Quarry (South-West Cameroon). *Applied and Environmental Soil Science*, *2024*(1), 8260177.

[17]. Kumar, S., & Sharma, R. K. (2024). Stability Analysis of Slope of a Pump House Building and Water Storage Tank at Narkanda, India: A case study. *Journal of Mining and Environment*, *15*(4), 1227-1240.

[18]. Mebrahtu, T. K., Heinze, T., Wohnlich, S., & Alber, M. (2022). Slope stability analysis of deep-seated landslides using limit equilibrium and finite element

methods in Debre Sina area, Ethiopia. *Bulletin of Engineering Geology and the Environment*, *81*(10), 403.

[19]. Varkey, D., Hicks, M. A., & Vardon, P. J. (2023). Effect of uncertainties in geometry, inter-layer boundary and shear strength properties on the probabilistic stability of a 3D embankment slope. *Georisk: Assessment and Management of Risk for Engineered Systems and Geohazards*, *17*(2), 262-276.

[20]. Yadav, D. K., Mishra, P., Jayanthu, S., & Das, S. K. (2022). On the application of IoT: slope monitoring system for open-cast mines based on LoRa wireless communication. *Arabian Journal for Science and Engineering*, *47*(2), 1387-1398.

[21]. Truong, P., & Loch, R. (2004, July). Vetiver system for erosion and sediment control. In *Proceeding of 13th international soil conservation organization conference* (pp. 1-6).

[22]. Gray, D. H., & Sotir, R. B. (1996). *Biotechnical and soil bioengineering slope stabilization: a practical guide for erosion control*. John Wiley & Sons.

[23]. Barker, D. (Ed.). (1995). *Vegetation and slopes: stabilisation, protection and ecology*. Thomas Telford.

[24]. Norris, J. E., Stokes, A., Mickovski, S. B., Cammeraat, E., Van Beek, R., Nicoll, B. C., & Achim, A. (Eds.). (2008). *Slope stability and erosion control: ecotechnological solutions*. Springer Science & Business Media.

[25]. Bureau of Indian Standards (1976) *IS 4968-1: Method for subsurface sounding for soils - Part 1 Dynamic cone penetration test*. New Delhi: Bureau of Indian Standards.

[26]. Bureau of Indian Standards (1976) *IS 8009-1: Code of practice for calculation of settlement of foundations - Part 1: Shallow foundations subjected to symmetrical static vertical loads*. New Delhi: Bureau of Indian Standards.

[27]. IS 1904 (1986): Code of practice for design and construction of foundations in soils: General requirements [CED 43: Soil and Foundation Engineering].

[28]. Bureau of Indian Standards (1973) *IS 2720-2: Methods of test for soils - Part 2: Determination of water content*. New Delhi: Bureau of Indian Standards.

[29]. Bureau of Indian Standards (1980) *IS 2720-3: Methods of test for soils - Part 3: Determination of specific gravity*. New Delhi: Bureau of Indian Standards.

[30]. Bureau of Indian Standards (1985) *IS 2720-5: Methods of test for soils - Part 5: Determination of liquid and plastic limit*. New Delhi: Bureau of Indian Standards.

[31]. IS 2720-11 (1993): Methods of test for soils, Part 11: Determination of the shear strength parameters of a specimen tested in unconsolidated undrained triaxial compression without the measurement of pore water pressure [CED 43: Soil and Foundation Engineering].

[32]. DR, G. (1987). Vegetation and slope stability. *Slope stability*, 187-230.

[33]. Asada, H., & Minagawa, T. (2023). Impact of vegetation differences on shallow landslides: A case study in Aso, Japan. *Water*, *15*(18), 3193.

[34]. Hoek, E., & Bray, J. D. (1981). *Rock slope engineering*. CRC press.

[35]. IS 1893: Part 1: 2016: Criteria for Earthquake Resistant Design of Structures - Part 1: General Provisions and Buildings.

[36]. Griffiths, D. V., & Lane, P. A. (1999). Slope stability analysis by finite elements. *Geotechnique*, *49*(3), 387-403.

[37]. Wolf, J. P. (1987). Soil-structure-interaction analysis in time domain. In *Structural mechanics in reactor technology*.

[38]. Kuhlemeyer, R. L., & Lysmer, J. (1973). Finite element method accuracy for wave propagation problems. *Journal of the soil mechanics and foundations division*, *99*(5), 421-427.

[39]. IS14243-2. Guidelines for selection and development of site for building in hill areas, Part 2: Selection and development. Bur. Indian Stand. N.Delhi, India, 1995.

[40]. IS 14458-1 (1998): Guidelines for retaining wall for hill area, Part 1: Selection of type of wall [CED 56: Hill Area Development Engineering].

[41]. Kumar, A., Sharma, R. K., & Mehta, B. S. (2020). Slope stability analysis and mitigation measures for selected landslide sites along NH-205 in Himachal Pradesh, India. *Journal of Earth System Science*, *129*(1), 135.

[42]. Khanna, R., & Dubey, R. K. (2021). Comparative assessment of slope stability along road-cuts through rock slope classification systems in Kullu Himalayas, Himachal Pradesh, India. *Bulletin of Engineering Geology and the Environment*, *80*(2), 993-1017.

# ارزیابی پایداری شیب یکپارچه و راه حل‌ها با استفاده از PLAXIS 2D و GEO5

**ساهیل تاکور* و راوی کومار شارما**

**گروه مهندسی عمران، موسسه ملی فناوری هامیرپور، هیماچال پرادش، هند**

ارسال ۲۰۲۴/۱۲/۰۹، پذیرش ۲۰۲۴/۰۳/۰۸

* نویسنده مسئول مکاتبات: sahilthakur94180@gmail.com

**چکیده:**

پایداری شیب برای ایمنی زیرساخت، به ویژه در مناطق لرزه‌ای فعال حیاتی است. این کار با استفاده از ترکیبی جدید از روش‌های تعادل حدی (LEMs) و روش‌های المان محدود (FEMs) پایداری یک شیب در امتداد جاده باروتی-ریور در هیماچال پرادش، واقع در منطقه ۵ را ارزیابی می‌کند. این تجزیه و تحلیل شرایط شیب طبیعی و تأثیر اقدامات کاهش پایدار، از جمله سازه‌های نگهدارنده و تکنیک‌های مهندسی زیستی را تحت شرایط استاتیک و دینامیکی بررسی می‌کند. مدل خاک مدول کشش (E)۹۰۰۰۰ کیلو نیوتن بر متر مربع و نسبت پواسون (v) ۰.۳ را برای انعکاس برهمکنش های شیب-خاک-ساختار واقع گرایانه گنجانده است. سازه های نگهدارنده مانند دیوارهای گرانشی، کنسول و گابیون (ارتفاع ۴ متر، ۶ متر و ۵ متر) با استفاده از فولاد M30 RCC و Fe500 ساخته شدند. اقدامات مهندسی زیستی شامل علف‌های ریشه‌دار مانند وتیور و چمن جارو برای بهبود انسجام خاک (c)، درختچه‌هایی مانند Lantana camara برای پایداری سطح و درختانی مانند Albizia lebbeck برای تقویت لایه‌های عمیق‌تر خاک بود. این مداخلات مبتنی بر پوشش گیاهی، انعطاف‌پذیری شیب را افزایش داد، در حالی که بازسازی اکولوژیکی را ارتقا داد. تجزیه و تحلیل LEM نظری ثبات حاشیه ای را با مقادیر FOS استاتیک ۱.۱ و FOS شبه استاتیک ۱.۰۵ نشان داد. تجزیه و تحلیل شبه استاتیک GEO5 مقدار FOS بسیار پایین ۰.۸۸ را برای شرایط اشباع دینامیکی نشان داد که با ساختارهای نگهدارنده به ۲.۰۱ بهبود یافت. تجزیه و تحلیل FEM با استفاده از PLAXIS 2D بینش‌های دقیق‌تری را ارائه می‌کند و تعاملات پیچیده ساختار خاک را با FOS ایستا ۱.۰۲۸ و FOS دینامیکی ۰.۹۹۴ ثبت می‌کند. با ترکیب FEM با استراتژی‌های کاهش پایدار، این کار چارچوبی برای تثبیت شیب انعطاف‌پذیر، تضمین ایمنی و در عین حال ارتقای پایداری زیست‌محیطی در مناطق لرزه‌ای فعال ارائه می‌دهد.

**کلمات کلیدی:** مدل سازی عددی; روش المان محدود (FEM)؛ فاکتور ایمنی (FOS).